

Interplay of superconductivity and magnetism in strong coupling.

C. N. A. van Duin and J. Zaanen

Institute Lorentz for Theoretical Physics, Leiden University

P.O.B. 9506, 2300 RA Leiden, The Netherlands

(May 16, 2017; E-mail:cvduin@lorentz.leidenuniv.nl; jan@lorentz.leidenuniv.nl)

A model is introduced describing the interplay between superconductivity and spin-ordering. It is characterized by on-site repulsive electron-electron interactions, causing antiferromagnetism, and nearest-neighbor attractive interactions, giving rise to d-wave superconductivity. Due to a special choice for the lattice, this model has a strong-coupling limit where the superconductivity can be described by a bosonic theory, similar to the strongly coupled negative U Hubbard model. This limit is analyzed in the present paper. A rich mean-field phase diagram is found and the leading quantum corrections to the mean-field results are calculated. The first-order line between the antiferromagnetic- and the superconducting phase is found to terminate at a tricritical point, where two second-order lines originate. At these lines, the system undergoes a transition to- and from a phase exhibiting both antiferromagnetic order and superconductivity. At finite temperatures above the spin-disordering line, quantum-critical behavior is found. For specific values of the model parameters, it is possible to obtain $SO(5)$ symmetry involving the spin- and the phase-sector at the tricritical point. Although this symmetry is explicitly broken by the projection to the lower Hubbard band, it survives on the mean-field level, and modes related to a spontaneously broken $SO(5)$ symmetry are present on the level of the random phase approximation in the superconducting phase.

71.27.+a, 74.72.-h, 75.10.-b, 74.25 DW

I. INTRODUCTION

Both for empirical- and historical reasons, research on superconductivity tends to be preoccupied with the weak coupling limit. From a more general perspective, BCS theory as well as Gorkov-Migdal-Eliashberg theory correspond with a special case which in a sense is pathological. The emphasis is completely on the amplitude of the order parameter while fundamentally superconductivity is about breaking of gauge symmetry, associated with the phase sector. The work of Schmitt-Rink and Nozieres [1] revealed that the BCS theory for a s-wave superconductor can be smoothly continued to the strong coupling limit. It is generally recognized that it is far easier to understand the vacuum structure of such a superconductor in strong coupling. Amplitude fluctuations can be regarded as highly massive excitations and all what remains is the phase sector described in terms of hard-core bosons, or alternatively in terms of pseudo-spin models.

In the context of high T_c superconductivity one encounters a far more complex physics. Abundant evidence is available for a d-wave superconducting order parameter. This is usually discussed in terms of weak-coupling theory with its d-wave nodal fermions while the more sophisticated approaches start from this limit, attempting to penetrate the intermediate coupling regime using self-consistent perturbation theory [2]. The obvious problem is that the coherence length is rather short [3]. At the same time, an interesting case has been presented claiming that much of the thermodynamics can be understood from phase-dynamics alone [4], completely disregarding

amplitude fluctuations. It would therefore be useful to study strong coupling theories for d-wave superconductors.

An even better reason to pursue a strong coupling perspective is the growing evidence for the presence of well developed antiferromagnetism coexisting with the superconductivity. Traditionally, this was approached within, again, an implicitly weakly coupled perspective. The magnetic fluctuations as seen in NMR and neutron scattering were believed to be due to the proximity to an amplitude driven spin density wave transition [5]. Recently, this perspective has been drastically changed due to the observation of strong static antiferromagnetic order associated with the stripe phases in the La_2CuO_4 system [6]. In the Nd doped samples where this order is strongest the magnitude of the Néel order parameter can be as large as $0.3 \mu_B$ [7], while $0.1 \mu_B$ has been claimed in ‘pristine’ $La_{1.88}Sr_{0.12}CuO_4$ [8]. It appears that this antiferromagnetic order is in competition or even coexisting with the superconducting order [8,9]. Given that the stripe antiferromagnet should be strongly renormalized downward due to transversal quantum spin fluctuations [10] the stripe antiferromagnet has to be strongly coupled. Given the strong similarities between the static order and the incommensurate spin fluctuations which seem to be generic for all cuprate superconductors in the underdoped regime, a strong coupling perspective on the antiferromagnetism should be closer to the truth even if static order is not present, at least as long as the doping is not too large.

Recently several theoretical attempts have been under-

taken to shed light on this problem of strongly coupled superconductivity and antiferromagnetism. The simplest theory of this kind is Zhang’s $SO(5)$ theory, where superconductivity and antiferromagnetism are ‘unified’ within a single larger symmetry [11]. Given that no such symmetry is manifestly present at the ultraviolet of the problem, this might well be misleading and one would like to have a more general framework in which this (near) $SO(5)$ symmetry appears as a special case. The manifest symmetry of the problem is $U(1) \times SU(2)$ (superconducting phase- and spin, respectively). The structure of the long wavelength effective theory based on this symmetry principle has been analyzed recently by one of the authors [12], including the charge order associated with the stripe phase. These approaches are only truly meaningful at long wavelength and a more complete understanding is in high demand. In fact, the only reasonably complete theory is the one by Vojta and Sachdev [13], based on the large N /small S saddle point of the $Spl(2N)$ t - J model. However, in this large N limit the antiferromagnetism is in the strongly quantum disordered regime, and is therefore at best dual to the renormalized classical Néel order of the stripe phases.

Here we will present an exceedingly simple toy model which seems nevertheless to catch much of the physics discussed in the above. It is similar in spirit to the lattice-boson description of superconductivity and magnetism discussed in Ref’s [14] and [15]. The pursuit is to construct a model which at the same time describes localized magnetism and local pairing superconductivity. The magnetism is undoubtedly related to strong, Hubbard U type on-site repulsions. This prohibits for obvious reasons on-site pairing. The next microscopic length scale available on the lattice is the lattice constant itself: the pairs causing the superconductivity live on the links of the lattice [16]. If such a link-pair is occupied, the sites connected by this link are both occupied by a single electron. In the presence of on-site repulsions these electrons will tend to turn into a spin system. The number fluctuations implied by the superconducting phase order correspond with such an occupied link-pair becoming unoccupied, causing at the same time a dilution of the spin system.

On the square lattice a subtlety keeps a theory with these link pairs as building blocks from being simple. Different from the large N limit with its spin-Peierls order [13], the link pairs cause both conceptual problems in describing the state at half-filling as well as serious technical problems. As will be discussed in Section II, a consistent formulation requires local constraints to be added to the theory in order to exclude tilings of the lattice characterized by multiple occupancies on the sites. This is not necessarily fatal: the theory is bosonic and it might well be that Jastrow projections cure the problem. A central result of this paper is our discovery of a different lattice where these likely non-essential ‘correlation’ problems are

absent: the $1/5$ depleted lattice shown in Fig. 1. The link-pairs live on the long bonds, while the short bonds only carry spin-spin interactions. As will be further discussed, this model is characterized by an unproblematic classical (in fact, large d) limit. This allows us to derive in a controlled way a complete semi-classical description.

As discussed in Section III, we find a surprisingly rich phase diagram on the classical level containing all phases, which have been up to now suggested in this context, including the large N spin-quantum paramagnets. Perturbing around this classical limit, we address the structure of the semiclassical theory including the universality classes at the various phase transitions (Section IV). By fine tuning parameters, we find lines in the phase diagram where the $SO(5)$ symmetry is approached. However, even at the most symmetric point $SO(5)$ is not reached: as we will show, the theory becomes $SO(5)$ symmetric on the classical level but the quantum corrections destroy this symmetry again. As was already pointed out in the context of the $SO(5)$ symmetric ladders, fine tuning of the on-site repulsions is required to stabilize the full symmetry (Sections V and VI).

II. THE MODEL

A. Correlated superconductivity

For the strong-coupling description we are aiming at, the microscopic building blocks are electron link-pairs, created by the operators

$$L_{i,\delta}^{\sigma_1\sigma_2\dagger} = c_{i,\sigma_1}^\dagger c_{i+\delta,\sigma_2}^\dagger, \quad (1)$$

where δ is a lattice unit-vector, while i labels the sites. Such a link-pair is the typical microscopic object in a strong-coupling theory of d-wave superconductivity and the smallest electron-pair that can support spin degrees of freedom. Two serious problems arise when trying to construct a model from these operators, one technical and one conceptual. The technical problem is related to the spatial structure of the link-pairs, which introduces correlations between pairs centered on different bonds. These correlations show up in the commutation relations of the link operators. Operators along different bonds do not commute if their links share a common site. As a result, the dimension of the link-operator algebra grows with the system size. This makes a simple pseudo-spin description of the charge-sector impossible and not much seems to have been gained by going to the strong-coupling limit.

This problem can be avoided by assuming that one can somehow keep track of which electrons belong to a particular pair (this can be ambiguous, for instance in the case of four electrons sitting in a square). If this is possible, the link-pairs can be described by hard-core

boson-operators, satisfying $b_{i,\delta}^{\sigma_1\sigma_2} b_{i,\delta'}^{\sigma_1\sigma_2\dagger} = 0$ for $\delta \neq \delta'$. Link-bosons on different bonds always commute, removing the problem of the infinite-dimensional link-algebra. The correlation effects then show up in a different way, however. The hard-core link-bosons are spinful generalizations of the quantum dimers [17] [18]. It is well known that even the classical theory of the dimers is a complex combinatorics problem, which was solved for the case of half-filling [19], but not for general densities. This problem seems unavoidable when one tries to construct a strong-coupling theory for electron-pairs with one or the other real space internal structure on the square lattice.

The conceptual problem is related to the fact that our link-pairs carry spin. It concerns the state at half-filling. On the square lattice, there are many ways in which the link-pairs can be distributed over the lattice to obtain complete covering. Since the half-filling state is a pure spin-system, this charge degree of freedom is superfluous. The link-pair model at half-filling therefore suffers from a large degeneracy.

In the large- N t - J model studied by Vojta and Sachdev [13], link-pairing arises as a result of nearest-neighbor spin-singlet formation, and the pairs are in this case spin-zero dimers. As a result, different link-pair configurations at half-filling correspond to different distributions of the singlet spin-bonds over the square lattice. These configurations are therefore physically distinct. The spin-Peierls order which is present at half-filling singles out a particular link-pair configuration, breaking the degeneracy.

For a large S type antiferromagnet, however, the spin-sector cannot be used to break the degeneracy associated with half-filling. Let us therefore consider a model where link-pairing arises as a result of charge-charge interactions. In this case, link-pairs can have both a singlet and a triplet spin-component, allowing for the construction of a half-filling antiferromagnet. Consider a nearest-neighbor attractive interaction V , an on-site repulsive interaction U and a longer-range repulsive interaction U' ,

$$\mathcal{H} = \sum_i \left[-V \sum_{\delta} n_i n_{i+\delta} + U n_{i\uparrow} n_{i\downarrow} + U' \sum_{\delta_1, \delta_2 \neq -\delta_1} n_i n_{i+\delta_1+\delta_2} \right] + \text{hopping processes}, \quad (2)$$

where δ runs over all lattice unit-vectors. The attractive interaction V promotes link-pairing, while the longer range repulsive interaction U' is needed to counteract phase-separation in the strong-coupling limit.

At small electron densities, the strong-coupling limit of the above model describes a dilute gas of electron link-pairs. Near half-filling, it describes a dilute gas of *hole* link-pairs, moving through a spin background. Taking hole-pairs and spins, instead of electron-pairs, as the elementary building blocks in the strong-coupling limit near half-filling, the large degeneracy in the description

is avoided. Such a perspective is not entirely satisfactory, however, since the spin-sector is in this case represented in a first-quantized form.

The technical problems, related to the spatial correlations between the link-pairs, of course remain also for this model. These correlations become important at finite densities away from zero- or half-filling, severely complicating the strong-coupling analysis of this model. Moreover, the short-range attractive and long-range repulsive interactions will give rise to charge ordering phenomena at intermediate densities, further complicating the physics.

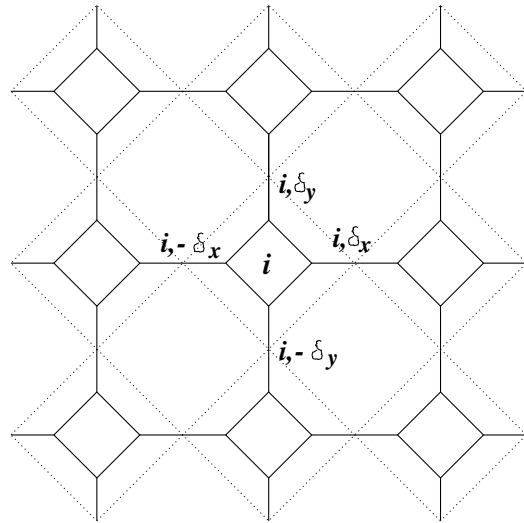


FIG. 1. The $\frac{1}{5}$ -depleted lattice. Dotted lines connect nearest-neighbor horizontal and vertical bonds.

B. Depleted lattice

The complex spatial correlations between link pairs and the tendency towards charge-ordering at intermediate densities as discussed in the previous subsection can be avoided by formulating the model not on the square lattice, but on the $1/5$ -depleted lattice, shown in Fig. 1. We arrive at this lattice by expanding the sites of a square lattice to form tilted squares. Along the bonds of the original square lattice, attractive charge-charge interactions are assumed, while on-site repulsive interactions are introduced to promote antiferromagnetism. The electron-Hamiltonian of such a model reads

$$\mathcal{H} = \sum_{i,\delta} \left[-V n_1^{i,\delta} n_2^{i,\delta} + U (n_{1\uparrow}^{i,\delta} n_{1\downarrow}^{i,\delta} + n_{2\uparrow}^{i,\delta} n_{2\downarrow}^{i,\delta}) \right] + \text{hopping processes}, \quad (3)$$

where the index i labels the square plaquettes, while (i, δ) denotes the four bonds extending from these plaquettes. The two sites connected by each long bond are numbered 1 and 2 from left to right and from bottom to top. The

hopping processes can include hopping along the long and the short bonds, as well as longer-range hopping across the square or the octagonal plaquettes. In the large V , large U limit, the above model reduces to one describing the physics of spinful link-pairs, which reside on the long bonds of the $1/5$ -depleted lattice. Note that the spatial correlations between these pairs are the same as between point-particles on a square lattice. Since the link-pairs on different long bonds do not share a common site, the algebra of the link-pairs on different bonds decouples and a pseudo-spin type description of the charge sector becomes possible. Admittedly, this amounts to a rather radical simplification as compared to the square lattice link-pair problem. However, the long wavelength physics we will derive for the depleted lattice might be of a greater generality because of the universality principle. In fact, we suspect that the complexities discussed in the previous subsection will add only tendencies towards charge ordering which can be to some extent discussed separately.

C. Pair-hopping and spin-spin interactions

Since the Hamiltonian Eq.(3) should be viewed as a toy-model, there is no reason to explicitly derive the strong-coupling description by starting from this Hamiltonian and integrating out the states with unpaired electrons. Instead, we simply formulate another toy-model, which describes generic features of the dynamics of bound link-pairs on the $1/5$ -depleted lattice. We include the minimal number of processes needed to capture the physics of such a system, making sure that the interactions are consistent with the symmetries of the lattice.

An antiferromagnetic spin-spin interaction J is assumed along the long bonds and a *ferromagnetic* interaction J_F along the short bonds. This choice allows for an extension of the model to higher dimensions without introducing frustration into the spin system, making it possible to reach the $d \rightarrow \infty$ limit and check the mean-field results there. For $J_F \gg J$, the half-filled system becomes equivalent to an $S = 2$ antiferromagnet on a square lattice (or $S = d$ on a d -dimensional hypercubic lattice). This property will be used to obtain an estimate of the quantum-corrections to the saddle-point results obtained in the next section.

A sublattice and an inter-sublattice hopping process are introduced, with amplitudes t_1 and t_2 . Both processes move a pair from a horizontal (vertical) bond to a nearest-neighbor vertical (horizontal) bond. The t_1 process respects the spin-ordering, keeping the electrons which form the pair on their original sublattice. The t_2 process moves the electrons from one sublattice to another, thereby frustrating Néel order.

Including a chemical potential μ , we arrive at the Hamiltonian

$$\mathcal{H} = \sum_i \left[\sum_{\sigma_1 \sigma_2} \left\{ t_1 \left(L_{i, \delta_x}^{\sigma_1 \sigma_2 \dagger} + L_{i, -\delta_x}^{\sigma_2 \sigma_1 \dagger} \right) \left(L_{i, \delta_y}^{\sigma_1 \sigma_2} + L_{i, -\delta_y}^{\sigma_2 \sigma_1} \right) + t_2 \left(L_{i, \delta_x}^{\sigma_1 \sigma_2 \dagger} + L_{i, -\delta_x}^{\sigma_2 \sigma_1 \dagger} \right) \left(L_{i, \delta_y}^{\sigma_2 \sigma_1} + L_{i, -\delta_y}^{\sigma_1 \sigma_2} \right) + \text{h.c.} \right\} - J_F \left(\vec{s}_{1i, \delta_x} + \vec{s}_{2i, -\delta_x} \right) \cdot \left(\vec{s}_{1i, \delta_y} + \vec{s}_{2i, -\delta_y} \right) + \sum_{\delta = \delta_x, \delta_y} \left(J \vec{s}_{1i, \delta} \cdot \vec{s}_{2i, \delta} - \mu n_{i, \delta} \right) \right], \quad (4)$$

where the same notation has been used as in Eq. (3). A projection operator $P_{i\delta} = (1 - n_{1\uparrow}^{i\delta} n_{1\downarrow}^{i\delta})(1 - n_{2\uparrow}^{i\delta} n_{2\downarrow}^{i\delta})$ has been included in the definition of the link-operators $L_{i\delta}^{\sigma_1 \sigma_2 \dagger}$, Eq. (1). This enforces the constraint of no double occupancy, which is a result of the large U limit in Eq.(3).

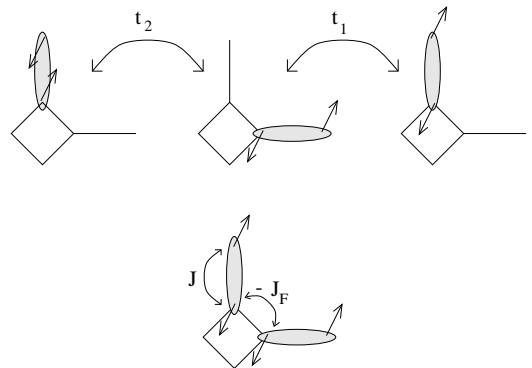


FIG. 2. Hopping processes and spin-spin interactions included in the model.

The Hilbert space on one long bond is spanned by five states: unoccupied (V), spin-singlet (A) and spin-triplet ($1, 0, -1$). The operators acting on this space are 5×5 matrices. Introducing the notation

$$(G_{ab})_{ij} = \delta_{i,a} \delta_{j,b}, \quad (5)$$

the pair creation operators can be written as:

$$\begin{aligned} L_{\uparrow\uparrow}^\dagger &= G_{1V}, \\ L_{\downarrow\downarrow}^\dagger &= G_{-1V}, \\ L_{\uparrow\downarrow}^\dagger &= \frac{1}{\sqrt{2}} (G_{0V} - G_{AV}), \\ L_{\downarrow\uparrow}^\dagger &= \frac{1}{\sqrt{2}} (G_{0V} + G_{AV}). \end{aligned} \quad (6)$$

These operators are the equivalent of the pseudo-spins which appear in the strong-coupling negative U Hubbard model [20]. The operators $G_{\alpha V}$, $G_{V\alpha}$ and $\frac{1}{2}(n_\alpha - n_V)$ form an $S = \frac{1}{2}$ spin-algebra ($\alpha = 1, 0, -1, A$). Pseudo-spins with a different spin-index α do not commute. In section V, the constraint of no double occupancy is abandoned to allow for the construction of an $SO(5)$ symmetric version of this model. The operators (6) then become

$S = 1$ pseudo-spins and operators with a different index α do commute in this case.

It is convenient to introduce the total spin and the Néel moment of a link-pair

$$\vec{S}_{i,\delta} = \vec{s}_{1i,\delta} + \vec{s}_{2i,\delta} \ ; \ \vec{\tilde{S}}_{i,\delta} = \vec{s}_{1i,\delta} - \vec{s}_{2i,\delta} \ , \quad (7)$$

which are given by

$$\begin{aligned} S^z &= G_{11} - G_{-1-1} \ , \\ S^+ &= \sqrt{2}(G_{10} + G_{0-1}) \ , \\ \tilde{S}^z &= -G_{A0} - G_{0A} \ , \\ \tilde{S}^+ &= \sqrt{2}(G_{1A} - G_{A-1}) \ , \end{aligned} \quad (8)$$

satisfying $SO(4)$ commutation relations. After absorbing a factor $(-1)^{i_x+i_y} \text{sign}(\delta)$ into the singlet-state $|A_{i,\delta}\rangle$, which induces a staggering of $\vec{\tilde{S}}$ and G_{AV} , the Hamiltonian takes the form

$$\begin{aligned} \mathcal{H} = \sum_i \sum_{\substack{\delta_1 = \pm\delta_x \\ \delta_2 = \pm\delta_y}} \left[(t_1 + t_2) \sum_{\alpha=1,0,-1} \left(G_{\alpha V}^{i,\delta_1} G_{V\alpha}^{i,\delta_2} + \text{h.c.} \right) \right. \\ \left. + (t_1 - t_2) \left(G_{AV}^{i,\delta_1} G_{VA}^{i,\delta_2} + \text{h.c.} \right) \right. \\ \left. - \frac{J_F}{4} \left(\vec{S}_{i,\delta_1} + \eta_i \vec{\tilde{S}}_{i,\delta_1} \right) \cdot \left(\vec{S}_{i,\delta_2} + \eta_i \vec{\tilde{S}}_{i,\delta_2} \right) \right] \\ + \sum_i \sum_{\delta=\delta_x,\delta_y} \left[\frac{1}{4} J \left(1 - n_V^{i,\delta} - 4n_A^{i,\delta} \right) - \mu \left(1 - n_V^{i,\delta} \right) \right] \ , \quad (9) \end{aligned}$$

where $\eta_i = (-1)^{i_x+i_y}$ is the AF staggering factor. Note that it cannot be absorbed into $\vec{\tilde{S}}_{i,\delta}$, since (i, δ_x) and $(i+1, -\delta_x)$ label the same bond.

III. MEAN-FIELD ANALYSIS

A variational Hartree-Fock procedure is used for the mean-field analysis. In the ansatz-wavefunction, the Néel-vector is fixed in the z - and the total spin in the x -direction ($\langle \vec{S} \rangle \cdot \langle \vec{\tilde{S}} \rangle = 0$). The pseudo-spin degrees of freedom of the charge/phase sector are described by an $S = \frac{1}{2}$ spin coherent state

$$|\theta, \psi; \tilde{\phi}^y, \chi\rangle = \sin\theta e^{-i\psi} |V\rangle + \cos\theta |\tilde{\phi}^y, \chi\rangle \ , \quad (10)$$

while the spin degrees of freedom of the pair are contained in $|\tilde{\phi}^y, \chi\rangle$

$$|\tilde{\phi}^y, \chi\rangle = e^{-i\tilde{\phi}^y \tilde{S}^y} (\cos\chi |A\rangle - \sin\chi |0\rangle) \ . \quad (11)$$

$|\tilde{\phi}^y, \chi\rangle$ is just the bilayer coherent state [21] where the global orientation of the two-spin system has been fixed.

We list the expectation-value of a number of quantities with respect to the variational state

$$\begin{aligned} n &= 1 - \langle n_V \rangle = \cos^2 \theta \ , \\ \langle S^x \rangle &= n \sin 2\chi \sin \tilde{\phi}^y \ ; \ \langle S^y \rangle = \langle S^z \rangle = 0 \ , \\ \langle \tilde{S}^z \rangle &= n \sin 2\chi \cos \tilde{\phi}^y \ ; \ \langle \tilde{S}^x \rangle = \langle \tilde{S}^y \rangle = 0 \ , \\ \langle n_A \rangle &= n \cos^2 \chi \cos^2 \tilde{\phi}^y \ . \\ \langle G_{\alpha V} \rangle &= \sqrt{n(1-n)} e^{-i\psi} \langle \tilde{\phi}^y, \chi | \alpha \rangle \ , \end{aligned} \quad (12)$$

where $\alpha = 1, 0, -1, A$ labels the four spin-states. The role which the various parameters play can be determined from this list: θ fixes the pair-density; $\tilde{\phi}^y$ determines the relative magnitude of $\langle \vec{S} \rangle$ and $\langle \vec{\tilde{S}} \rangle$, while their total magnitude is fixed by χ ; ψ represents the phase which orders in the superconducting state.

The variational energy is given by

$$E_{\text{var.}}(\{\theta, \psi; \tilde{\phi}^y, \chi\}_{i,\delta}) = \langle \{i, \delta\} | \mathcal{H} | \{i, \delta\} \rangle \ , \quad (13)$$

where

$$|\{i, \delta\}\rangle = \prod_{i,\delta} |\theta, \psi; \tilde{\phi}^y, \chi\rangle_{i,\delta} \ . \quad (14)$$

In the mean-field analysis, it is assumed that the staggered local magnetization and the charge density are uniform. The phase ψ_l is allowed to have a different value on horizontal (ψ^H) and vertical bonds (ψ^V). We then arrive at the following mean-field energy

$$\begin{aligned} E_{\text{MF}} &= N \left(\sin^2 2\theta (t_1 + t_2 - 2t_2 \cos^2 \chi \cos^2 \tilde{\phi}^y) \times \right. \\ &\times \cos(\psi^H - \psi^V) - \frac{1}{2} J_F \cos^4 \theta \sin^2 2\chi \\ &\left. + \frac{1}{4} J \cos^2 \theta (1 - 4 \cos^2 \chi \cos^2 \tilde{\phi}^y) - \mu \cos^2 \theta \right) \ , \quad (15) \end{aligned}$$

where N denotes the number of long bonds. Minimizing Eq. (15), a variety of mean-field groundstates is obtained as a function of the various parameters. The results are summarized in figures 3-5 and in table 1. We focus here on the case $t_1 > 0$, for which the superconducting state is typically of d-wave type ($\psi^H - \psi^V = \pi$). The same phase-diagram results for $t_1 \rightarrow -t_1$ and $t_2 \rightarrow -t_2$, but with s-wave instead of d-wave phase-order. For simplicity, J , t_1 , t_2 and μ are expressed in units of J_F from here on.

At half-filling, the physics is determined by the competition between the antiferromagnetic and the ferromagnetic spin-spin interaction. While the first promotes singlet-formation along the horizontal and vertical bonds, the second favors large local magnetic moments. J therefore tunes the singlet density in the groundstate at half-filling. For $J \ll 1$, the system has full Néel order with $\langle n_A \rangle = \frac{1}{2}$, $|\langle \vec{\tilde{S}} \rangle| = 1$. The singlet density increases linearly with J up to $\langle n_A \rangle = 1$ at $J = 2$, where the staggered magnetization vanishes in a second order transition to a quantum paramagnet phase (Fig. 3).

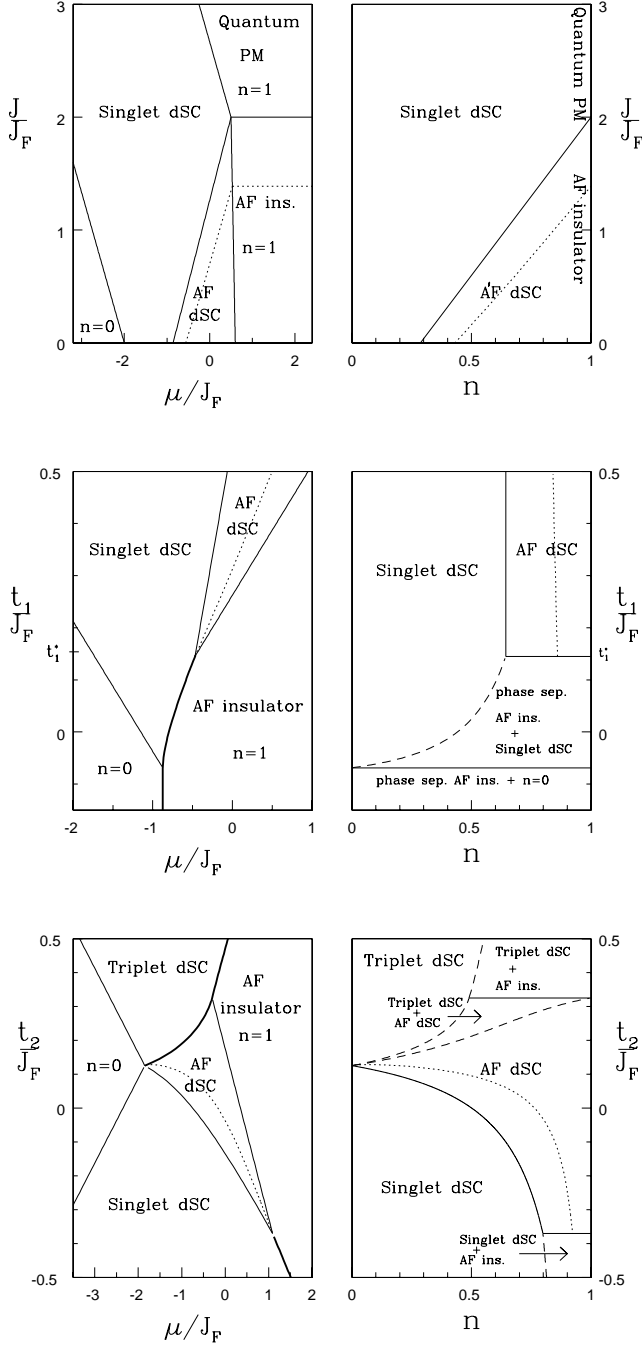


FIG. 3. Mean field phase diagram of J versus μ and n , for $t_1 > t_1^*$ ($t_1 = 0.4J_F$, $t_2 = -0.1J_F$). Bold lines indicate first order transitions. At the dotted line, transversal quantum spin-fluctuations destroy the antiferromagnetic order.

FIG. 4. Mean field phase diagram of t_1 versus μ and n , for $J < 2J_F$ and $t_2 < J/8$ ($J = J_F$, $t_2 = -0.1J_F$).

FIG. 5. Mean field phase diagram of t_2 versus μ and n , for $J < 2J_F$ and $t_1 > (4J_F^2 + J^2)/32J_F$ ($t_1 = 0.4J_F$, $J = J_F$).

For densities smaller than one, the two hopping processes begin to play a role. Since the case of a uniform charge-distribution is considered and since all electrons are paired in the strong-coupling limit, all variational states with a non-integer electron-density exhibit superconductivity. The superconducting order-parameter depends on the electron-density as $|\Delta| \sim \sqrt{n(1-n)}$, see Eq.(12).

The value of the hopping amplitude t_1 determines the nature of the transition from the antiferromagnetic insulator at half-filling to the singlet superconductor at lower densities. For small t_1 , this transition is first order as a function of μ , giving rise to a region of antiferromagnet/ superconductor phase separation in the t_1 - n phase-diagram (Fig. 4). At $t_1 = t_1^* = \frac{1}{8} + 2t_2^2$, the first order line splits into two second order lines. A region opens up in which the system has both antiferromagnetic spin order and superconductivity. In this antiferromagnetic superconductor (AFSC) phase, the electrons which carry the superconducting order-parameter are at the same time responsible for the antiferromagnetism. This state is most easily visualized by thinking of a small density of nearest-neighbor hole-pairs being doped into a half-filling antiferromagnet. If these hole-pairs are most mobile along the diagonals of the square lattice, where their movement does not disturb the AF spin order, they can delocalize and in that way give rise to superconductivity *without* at the same time destroying the antiferromagnetic order. The condition that diagonal pair-hopping has to dominate to get an AFSC-phase on the square lattice is reflected by the condition $t_1 > t_1^*$ for the present model.

There are three ways in which the spin order-parameter in the AFSC phase is suppressed through the doping with hole-pairs. The simplest one corresponds with the dilution of the antiferromagnet by the removal of spins. More interestingly, the inter-pair spin-spin interaction J_F scales with the pair-density squared, while the intra-pair spin-spin interaction J scales linearly with n . As a result, the ferromagnetic interaction is suppressed by a factor n relative to J , pushing the ratio J/J_F closer to its critical value and reducing the magnetic moment per pair. Finally, the hopping process t_2 frustrates the Néel order, provided that $sign(t_2) = -sign(t_1)$ (the other case is discussed below). The increase of the singlet density per pair due to the last two processes results in a transition to the singlet superconductor at $n = n_c = \frac{J-8t_2}{2-8t_2}$.

Since the t_2 process amounts to a t_1 -type hop with an additional interchange of the two electrons forming the pair, it picks up a minus-sign when acting on a pair in the antisymmetric spin-singlet state. Suppose that t_1 and t_2 have the same sign. A singlet-pair, through the t_2 -process, then frustrates the phase-ordering as favored by the t_1 -hop. To reduce this frustration, the singlet

content of the pairs is suppressed as t_2 is increased, enhancing the spin-ordering in the AFSC phase. Eventually, a first order transition occurs to a ferromagnetically ordered triplet superconductor phase, where the singlet-density is reduced to zero (Fig.5).

If t_1 and t_2 have opposite sign, the *triplet* component is suppressed through the same process and the t_2 -hop reduces the spin-order in the AFSC phase. Note that t_2 causes a positive shift of the critical value t_1^* regardless of its sign. This reflects the fact that on-sublattice hopping must dominate in order for an AFSC phase to occur ($t_1 > t_1^*$ implies $t_1 \geq |t_2|$, where the equal sign occurs for $|t_2| = \frac{1}{4}$).

It should be verified that the saddle-point solution becomes exact in the limit $d \rightarrow \infty$. To reach this limit, the model has to be formulated in arbitrary dimension. The d-wave phase order then poses a problem, since it cannot be generalized to dimensions higher than 2. However, the Hamiltonian of the 2d system is invariant under a simultaneous sign-change of t_1 , t_2 and $G_{\alpha V}^{i, \pm \delta_x}$, which implies that d- and s-wave order are equivalent for the 2d model¹. We therefore flip the sign of t_1 and t_2 and study the $d \rightarrow \infty$ limit for the s-wave ordered state. In order to keep the energy finite, J_F , t_1 and t_2 are scaled with $\frac{1}{d}$ while taking the limit. The variation of the energy is found to be of order $\frac{1}{d}$ for the saddle-point solution. Since it vanishes at large d , the mean-field groundstate indeed becomes an eigenstate of the system in this limit.

phase	n	$\cos 2\chi$	$\cos \phi^y$
Spin-liquid	1	1	1
Néel dSC	$\frac{-J-4\mu-16t_1-8Jt_2+64t_2^2}{4(1-8t_1+16t_2^2)}$	$\frac{J+8t_2(n-1)}{2n}$	1
Singlet dSC	$\frac{4\mu+16(t_1-t_2)+3J}{32(t_1-t_2)}$	1	1
Triplet dSC	$\frac{J-4\mu-16(t_1+t_2)}{4-32(t_1+t_2)}$	0	0
AF	1	$\frac{J}{2}$	1

TABLE 1: Mean-field results for the various phases.

IV. TRANSVERSAL SPIN FLUCTUATIONS

In the AFSC phase, both the $U(1)$ phase- and the $SU(2)$ spin-symmetry are spontaneously broken. As a result, the system has two spin-wave modes and one phase Goldstone mode. These gapless modes dominate its long-wavelength physics. Since they decouple, the phase and spin degrees of freedom of the system may be treated separately at sufficiently large lengthscales.

The physics of the phase sector is equivalent to that of an XY-spin model in an external magnetic field, which has a dynamical critical exponent $z = 2$. The $T = 0$ system is therefore effectively at its upper critical dimension $d = 2 + z = 4$. Because of the high effective dimensionality, phase-fluctuations only give small correction to the zero-temperature mean-field results for the insulator-superconductor transition [22].

The long-wavelength behavior of the spin-sector in the AFSC phase is characterized by a critical exponent $z = 1$. Hence, at $T = 0$, the spin-sector lives effectively in three dimensions and fluctuation-effects can be significant. The long-wavelength spin physics is described by an effective non-linear sigma model [23,24]. This model contains one coupling constant, g_0 , which is a measure of the quantum fluctuations in the system. At a critical value of g_0 , the spin-system undergoes a quantum phase transition from a Néel ordered state to a quantum paramagnet. For the present model, g_0 is expected to diverge at the mean-field transitions to the singlet superconductor and the paramagnetic insulator [21]. Transversal fluctuations are therefore expected to significantly reduce the region in the phase-diagram where AF order is stable.

The coupling constant of the effective non-linear sigma model depends on the bare values of the spin stiffness and the perpendicular susceptibility, which are properties of the microscopic model. The mean-field expressions for these quantities can serve as an estimate for their bare value [21]. These expressions are derived below for the present model.

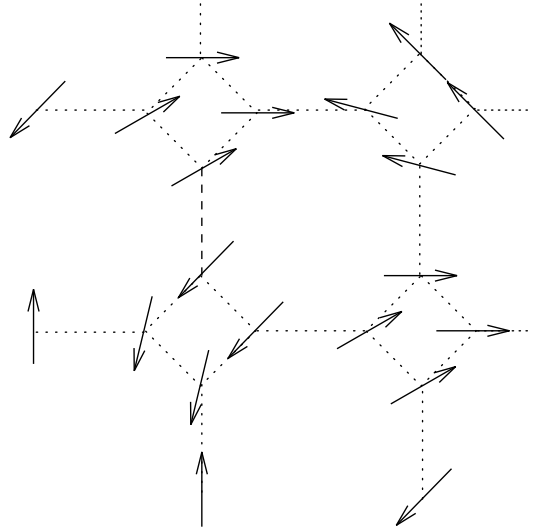


FIG. 6. A spin-configuration with a twist along the $x + y$ -direction.

¹This no longer holds if longer-range hopping processes are included.

We define the perpendicular susceptibility as the induced magnetization per square plaquette (containing four spins) by a vanishing magnetic field applied perpendicular to the direction of antiferromagnetic ordering. It is calculated by adding a magnetic field term to the mean-field energy Eq. (15),

$$H \sum_{i,\delta=\delta_x,\delta_y} \langle S_{i,\delta}^x \rangle = NH \cos^2 \theta \sin 2\chi \sin \tilde{\phi}^y \quad (16)$$

and subsequently minimizing the energy. This yields

$$\chi_{\perp} = \lim_{H \rightarrow 0} \frac{2 \langle S^x \rangle}{H} = \frac{2(1 - \cos 2\chi)n}{J - 8t_2(1 - n)} \Rightarrow \begin{cases} \chi_{\perp}^{\text{AF}} = \frac{2-J}{J} \\ \chi_{\perp}^{\text{AFSC}} = \frac{n(2-8t_2)-J+8t_2}{J-8t_2(1-n)} \end{cases} \quad (17)$$

The susceptibility vanishes at the transitions to the quantum paramagnet and the singlet superconductor phase. It has a divergence at $n = 1 - \frac{J}{8t_2}$, which is interrupted by the first order transition to the triplet superconductor phase (Fig. 5) (the line where χ_{\perp} diverges and the first-order line approach each other for small n).

For $n = 1$ and $J_F \gg J$, the four spins around each square plaquette lock into a symmetric state. The spin-operators can then be replaced by $\frac{1}{4}$ times the total spin-operator on the plaquette. The resulting Hamiltonian describes an $S = 2$ antiferromagnet on a square lattice, with a spin-spin coupling $J_{\text{eff}} = \frac{1}{16}J$. Such a system has a mean-field perpendicular susceptibility $\chi_{\perp} = 1/8J_{\text{eff}} = 2/J$ [23] (where the lattice-spacing, in this case the distance between neighboring square plaquettes, is set to one). The above result for the susceptibility indeed reduces to this expression for $n = 1$ and $J \ll 1$.

To determine the spin stiffness, the configuration shown in Fig. 6 is considered. It has a slow twist in the spin order parameter along the $x + y$ -direction. The stiffness gives the lowest-order correction to the groundstate energy due to this twist [25].

At each antiferromagnetic bond along the direction of the twist, the spins have been rotated over an angle $\alpha \delta\phi$ in the XZ-plane, at each ferromagnetic bond over an angle $(1 - \alpha) \delta\phi$. This configuration is described by the variational state Eq. (10), where the spin-part is given by

$$e^{i l \delta\phi S^y} \left| \tilde{\phi}^y = \frac{1}{2} \alpha \delta\phi, \chi = \chi_{MF} \right\rangle, \quad (18)$$

with the index l labelling the bonds along the twist.

The antiferromagnetic interaction energy of this state is given by (compare with last line in Eq.(15))

$$\frac{1}{4} J N \cos^2 \theta \left(1 - 4 \cos^2 \chi \cos^2 \left(\frac{1}{2} \alpha \delta\phi \right) \right) \simeq E_{AF}(\delta\phi = 0) + \frac{1}{4} J N \alpha^2 \delta\phi^2 \cos^2 \theta \cos^2 \chi, \quad (19)$$

while the ferromagnetic energy is simply reduced by a factor $\cos(1 - \alpha) \delta\phi$ per twisted ferromagnetic bond. The phase-ordering energy also contributes to the spin stiffness. Along the twist, we have (d-wave order)

$$\begin{aligned} & \sum_{\alpha=1,0,-1} \langle G_{\alpha V}^l \rangle \langle G_{\alpha V}^{l+1} \rangle = \\ & - \sum_{\alpha=1,0,-1} \frac{1}{4} \sin^2 2\theta \langle \vec{\Omega} | e^{-i l \delta\phi S^y} | \alpha \rangle \langle \alpha | e^{i(l+1) \delta\phi S^y} | \vec{\Omega} \rangle = \\ & - \frac{1}{4} \sin^2 2\theta \langle \vec{\Omega} | (1 - |A\rangle \langle A|) e^{i \delta\phi S^y} | \vec{\Omega} \rangle \simeq \\ & - \langle G_{AV}^l \rangle \langle G_{VA}^{l+1} \rangle - \frac{1}{4} \sin^2 2\theta \left(1 - \frac{1}{2} \delta\phi^2 \underbrace{\langle \vec{\Omega} | S^y{}^2 | \vec{\Omega} \rangle}_{\sin^2 \chi} \right), \\ & \langle G_{AV}^l \rangle \langle G_{VA}^{l+1} \rangle = \\ & - \frac{1}{4} \sin^2 2\theta \cos^2 \chi \cos^2 \left(\frac{1}{2} \alpha^2 \delta\phi^2 \right) \simeq \\ & - \frac{1}{4} \sin^2 2\theta \cos^2 \chi \left(1 - \frac{1}{4} \alpha^2 \delta\phi^2 \right). \end{aligned} \quad (20)$$

Taking these contributions together, the energy-increase due to the twist in the spin order-parameter is found to be

$$\Delta E = \frac{1}{8} N \delta\phi^2 \left(2 \sin^2 2\theta [(t_1 + t_2) \sin^2 \chi - t_2 \alpha^2 \cos^2 \chi] + \sin^2 2\chi \cos^4 \theta (1 - \alpha)^2 + 2J \alpha^2 \cos^2 \theta \cos^2 \chi \right) \quad (21)$$

The distribution of the total twist over the two types of bonds is obtained by minimizing this energy with respect to α , which yields

$$\alpha_0 = \frac{n(1 - \cos 2\chi)}{n(1 - \cos 2\chi) + J - 4t_2(1 - n)}. \quad (22)$$

For J_F much larger than J and t_2 (or just J for $n = 1$), the twist is entirely localized on the antiferromagnetic bonds, as expected. At the transition to the spin disordered phases, it is localized on the ferromagnetic bonds.

The stiffness now follows from

$$\Delta E(\alpha_0) = \frac{N}{2} \delta\phi^2 \rho_s. \quad (23)$$

For the half-filling antiferromagnet, we obtain

$$\rho_s^{\text{AF}} = \frac{1}{8} J(2 - J), \quad (24)$$

while for the AFSC phase the stiffness is given by

$$\rho_s^{\text{AFSC}} = \frac{n(2 - 8t_2) - J + 8t_2}{8J + 16n} \times [2Jn + J^2 + 4(1 - n)(J(t_1 - 2t_2) + 2t_1n + 8t_2^2(1 - n))]. \quad (25)$$

Like the susceptibility, the stiffness vanishes at the transition to a spin-disordered phase. It reduces to the $S=2$, $J_{\text{eff}} = \frac{1}{16}J$ -form for $J \gg J_F$ at half-filling.

The bare coupling constant of the non-linear sigma model is given by $g_0 = (\rho_s \chi_{\perp})^{-\frac{1}{2}}$. As expected, it diverges at the transitions to the singlet superconductor and quantum paramagnet, since both the susceptibility and the stiffness vanish in these phases. In order to obtain a more precise estimate of g_0 , its value is shifted by a constant factor such that it agrees with the result for the $S=2$ antiferromagnet at $n = 1$, $J_F \gg J$. The bare coupling for the square lattice $S=2$ antiferromagnet can be determined from spin-wave results for the renormalized spin-wave velocity and perpendicular susceptibility, using the one-loop expression [24]

$$\frac{g_0}{4\pi} = \frac{1}{1 + 4\pi\chi_{\perp}c/\hbar\Lambda}, \quad (26)$$

where $\Lambda = 2\sqrt{\pi}/a$, with a the lattice spacing. Using the spin-wave results of Igarashi [25], we obtain

$$g_0^{S=2} \simeq 3.85. \quad (27)$$

For the half-filling antiferromagnet, the bare coupling constant is given by

$$g_0 = g_0^{S=2} \frac{2}{2 - J}, \quad (28)$$

while we find for the AFSC phase,

$$g_0 = g_0^{S=2} \frac{2\sqrt{(2n+J)(J-8t_2(1-n))}}{n(2-8t_2) - J + 8t_2} \times \frac{1}{\sqrt{2nJ + J^2 + 4(1-n)[J(t_1 - 2t_2) + 2t_1n + 8t_2^2(1-n)]}}. \quad (29)$$

The order-disorder transition at $g_0 = g_c = 4\pi$ is indicated by a dotted line in the mean-field phase diagrams, Figs 3-5. It is found that transversal spin fluctuations significantly reduce the parameter-range over which the Néel-ordered phases are stable, without changing the topology of the zero-temperature phase diagram.

At non-zero but low temperatures, the quantum non-linear sigma model predicts $z = 1$ quantum critical behavior in a parameter region around the AFSC to SC transition line [24]. The width of this region grows as $|g_0 - 4\pi| \sim T^{-\nu}$, with $\nu = 0.7$ the correlation-length critical exponent of the 3d Heisenberg model. This type of finite temperature behavior, where temperature becomes the only energy-scale in the system, has been reported for the underdoped cuprates by a number of authors [26–28].

Finally, we note that in the present model the superconductivity onset-temperature is completely determined by phase-fluctuations. This is a trivial consequence of the fact that we focussed on the strong-pairing limit. Nevertheless, it is consistent with recent analyses of the dependence of T_c on the zero-temperature phase-stiffness

and on the number of closely-spaced layers in the superconductor material, which point to a dominant role of finite-temperature phase-fluctuations in determining T_c [29].

V. $SO(5)$ SYMMETRIC POINT

The AFSC phase has an interesting property. Let us consider the $SO(5)$ superspin-vector [11] for this model.

$$\vec{N}_P = \left(\frac{1}{2}(G_{AV} + G_{VA}), \frac{1}{2}\vec{S}, \frac{1}{2i}(G_{AV} - G_{VA}) \right). \quad (30)$$

The label ‘P’ indicates that \vec{N}_P is defined in the projected Hilbertspace, where double site-occupancy is forbidden. The mean-field expectation value of \vec{N}_P satisfies

$$\left. \frac{\partial \langle \vec{N}_P \rangle^2}{\partial n} \right|_{t_2 = -\frac{1}{4}} = 0. \quad (31)$$

Hence, at the mean-field level and for this particular choice of t_2 , the AFSC phase can be characterized by an $SO(5)$ order-parameter which has components both in the superconducting and in the antiferromagnetic subspace, and which is rotated from the AF to the SC direction as the hole-density is increased. As one approaches the tricritical point, the AFSC states with different n become degenerate (Fig.3) and the mean-field state becomes invariant under rotations of \vec{N}_P . For $t_2 = -\frac{1}{4}$ the tricritical-critical point is located at $t_1 = t^* = \frac{1}{4}$, $\mu = \mu^* = \frac{J}{4}$.

It should perhaps come as no surprise that we find a ‘mean-field $SO(5)$ symmetry’ for this model. The special lattice used here has two orbitals per unit cell, which seems to be one of the requirements for constructing an $SO(5)$ symmetric model with short-range interactions [30]. This can be understood from the fact that the minimum number of sites required for the electron Hilbertspace in which an $SO(5)$ representation can be constructed is two (since the π -operators are spin-1, charge 2 objects). Two-leg spin ladders have a natural two-site unit, the rung, on which the $SO(5)$ order parameter can be defined. The lattice used here also has such a unit: the long bond. To formulate a short-range $SO(5)$ model on the square lattice, one either has to break the lattice-symmetry, or to involve a certain amount of coarse-graining, which means that the resulting $SO(5)$ -description is effective rather than microscopic.

In the following, an exact $SO(5)$ symmetric point is derived for the present model. The procedure used is similar to that for the $SO(5)$ symmetric ladder [31]. At the mean-field $SO(5)$ -point, the Hamiltonian is given by

$$\mathcal{H} = \mathcal{H}_0 + \mathcal{H}_1, \quad (32)$$

where

$$\mathcal{H}_0 = - \sum_i \sum_{\substack{\delta_1 = \pm\delta_x \\ \delta_2 = \pm\delta_y}} \vec{N}_P^{i,\delta_1} \cdot \vec{N}_P^{i,\delta_2} - J \sum_i \sum_{\delta=\delta_x,\delta_y} n_A^{i,\delta}, \quad (33)$$

$$\begin{aligned} \mathcal{H}_1 = \sum_i \sum_{\substack{\delta_1 = \pm\delta_x \\ \delta_2 = \pm\delta_y}} \frac{1}{4} \left[\vec{S}_{i,\delta_1} \cdot \vec{S}_{i,\delta_2} \right. \\ \left. + \eta_i \left(\vec{S}_{i,\delta_1} \cdot \vec{S}_{i,\delta_2} + \vec{S}_{i,\delta_1} \cdot \vec{S}_{i,\delta_2} \right) \right], \quad (34) \end{aligned}$$

absorbing a d-wave staggering into the $|V_{i,\delta}\rangle$ -state.

The second term, \mathcal{H}_1 , is manifestly not invariant under rotations of \vec{N}_P . After decoupling the operators on different bonds with respect to the order-parameters for superconductivity and antiferromagnetism, this term vanishes and therefore the symmetry breaking does not show up at the mean-field level. As Eder *et al.* pointed out [14], the first and the fourth component of \vec{N}_P are rotated into each other by transforming the zero-magnetization triplet state $|0\rangle$ into the hole-pair state $|V\rangle$. This transformation leaves the singlet density n_A invariant. Since one may assume in mean-field that all components of $\langle \vec{N}_P \rangle$ vanish except the first and the fourth (spontaneous symmetry breaking selects a preferred direction in the spin and phase sector) the decoupled mean-field Hamiltonian is invariant under this transformation. This implies that the $d \rightarrow \infty$ $SO(5)$ -symmetry is not only present in the zero-temperature groundstate, but also at finite temperatures, where higher energy-levels are thermally occupied.

As a first step towards an $SO(5)$ -symmetric Hamiltonian, \mathcal{H}_1 is subtracted from \mathcal{H} . This introduces second- and third-neighbor spin-spin interactions into the model.

The second term in \mathcal{H}_0 is an $SO(5)$ -invariant (this is discussed below). The first term is invariant under rotations of \vec{N}_P , but this does not imply that it is $SO(5)$ symmetric. There is no representation of the $SO(5)$ algebra on the projected Hilbertspace under which \vec{N}_P transforms as a vector. The rotation-symmetry is therefore broken at the quantum level. In a recent article [15], Zhang *et al.* show that mean-field $SO(5)$ symmetry always remains when a projection to the lower Hubbard band is applied to a system with full $SO(5)$ symmetry. Here we work backwards: mean-field $SO(5)$ -symmetry being established, we deduce a model with full $SO(5)$ symmetry by lifting the constraint of no double site-occupancy.

The basis of the single-bond Hilbert-space is extended to include the doubly occupied state $|D\rangle$. It now consists of one $SO(5)$ singlet (A) and one $SO(5)$ quintet (spin-triplet, D and V). The details of this representation of the $SO(5)$ algebra are briefly discussed in appendix A. We introduce an on-site repulsion $U \sum_{i\delta} n_{D i\delta}$. The general Hamiltonian on the unprojected Hilbert space is given by

$$\begin{aligned} \mathcal{H} = \sum_i \sum_{\substack{\delta_1 = \pm\delta_x \\ \delta_2 = \pm\delta_y}} \left[4(t_1 + t_2) \sum_{\alpha} \vec{\pi}_{i,\delta_1}^{\alpha} \cdot \vec{\pi}_{i,\delta_2}^{\alpha} \right. \\ \left. + (t_1 - t_2) \vec{\Delta}_{i,\delta_1} \cdot \vec{\Delta}_{i,\delta_2} \right. \\ \left. + \frac{1}{4} \left(\vec{S}_{i,\delta_1} + \eta_i \vec{S}_{i,\delta_1} \right) \cdot \left(\vec{S}_{i,\delta_2} + \eta_i \vec{S}_{i,\delta_2} \right) \right] \\ - \sum_{i,\delta=\delta_x,\delta_y} \left[J n_A^{i,\delta} + \left(\frac{J}{4} - U + \mu \right) n_D^{i,\delta} - \left(\mu - \frac{J}{4} \right) n_V^{i,\delta} \right], \quad (35) \end{aligned}$$

where $\vec{\Delta} = (\text{Re}\Delta, \text{Im}\Delta)$, $\vec{\pi}^{\alpha} = (\text{Re}\pi^{\alpha}, \text{Im}\pi^{\alpha})$ (see appendix A). The value of U has to be fine-tuned in order to obtain $SO(5)$ symmetry on a single bond. The resulting constraint is $\mu = \frac{J}{4}$ as before, but in addition $U = \frac{J}{2}$. Note that this is more restrictive than the local constraint for the ladder model [31], which leaves two free parameters. Since we only consider states of paired electrons, this model has fewer local $SO(5)$ invariants than the ladder.

To establish $SO(5)$ symmetry of the inter-pair interactions, one now has to take $t_1 = -t_2 = \frac{1}{8}$. After subtraction of \mathcal{H}_1 , this yields the Hamiltonian

$$\mathcal{H}_{SO(5)} = -\frac{1}{4} \sum_{\langle l,m \rangle} \vec{N}_l \cdot \vec{N}_m - J \sum_l n_A^l, \quad (36)$$

where l and m run over the square lattice spanned by the long bonds (dotted lines in Fig.1). The unprojected $SO(5)$ superspin \vec{N} is given by Eq. (A1). The local $SO(5)$ invariant n_A is related to the length of the superspin through $\vec{N}^2 = 1 + 4n_A$.

Note that Eq.(36) is not the most general $SO(5)$ -symmetric Hamiltonian which could be formulated. In principle, there can be an additional term of the form

$$\begin{aligned} \lambda \sum_{\langle l,m \rangle} \sum_{a < b} L_{ab}^l L_{ab}^m = \lambda \sum_{\langle l,m \rangle} \left[\sum_{\alpha} \vec{\pi}_l^{\alpha} \cdot \vec{\pi}_m^{\alpha} \right. \\ \left. + \vec{S}_{i,\delta_1} \cdot \vec{S}_{i,\delta_2} + Q_{i,\delta_1} Q_{i,\delta_2} \right], \quad (37) \end{aligned}$$

which is also an $SO(5)$ invariant. The charge-charge interaction $Q_{i,\delta_1} Q_{i,\delta_2}$ was omitted from the present analysis and a term of this form therefore does not appear at the symmetric point.

The projected $SO(5)$ ($pSO(5)$) symmetry at $U \rightarrow \infty$ evolves from the true $SO(5)$ symmetric point at fine-tuned U in the following way. Let us assume we have $t_1 = -t_2 = t$ and $U = \frac{J}{2} + \bar{U}$.

$$\begin{aligned} \mathcal{H} = - \sum_{\langle l,m \rangle} \left(2t \vec{\Delta}_l \cdot \vec{\Delta}_m + \frac{1}{4} \vec{S}_l \cdot \vec{S}_m \right) \\ + \sum_l \left(\bar{U} n_D^l - J n_A^l \right). \quad (38) \end{aligned}$$

The superspin has no preferred global direction for $\bar{U} = 0$, $t = \frac{1}{8}$. Since the AF groundstate does not have a $|D\rangle$

component, while the SC does, a small positive \bar{U} will flop the superspin to the AF direction. The energy-difference between the AF and the SC state can be compensated by an increase in t . For $\bar{U} \rightarrow \infty$, this procedure shifts the superspin-flop point from $t = \frac{1}{8}$ to $t = \frac{1}{4}$, with the SC groundstate now having $\langle n_D \rangle = 0$. The shift in t is accounted for by the different relative normalization of $\vec{\Delta}$ and \vec{S} in the definitions of \vec{N}_P and \vec{N} .

VI. COLLECTIVE MODES

In the above, it was shown that the inter-sublattice hopping t_2 , which couples the spin- and charge-dynamics in our model, plays a crucial role in establishing the $SO(5)$ -symmetry. This symmetry only emerges at the mean-field level for a specific value of t_2 . To further investigate the role of this hopping process, the collective modes in the antiferromagnetic and spin-disordered phases are analyzed. For $t_2 = 0$, it is found that a decoupled spin/charge perspective suffices to understand these modes, as one would expect. In this case, the superconductivity does not affect the collective spin-modes of the system.

This changes for non-zero t_2 . Although the dispersion-relations do not change qualitatively, the interpretation of the modes does. Most strikingly, the gapped spin-magnon mode of the Singlet SC phase acquires a π -mode component. This mode softens at the transition to the AFSC phase and becomes a pure, acoustic π -mode as the system is tuned towards p $SO(5)$ -symmetry.

The mode-spectrum for systems with p $SO(5)$ -symmetry was analyzed by Zhang *et al.* [15]. We reproduce their results for the present model and investigate the influence of further $SO(5)$ symmetry-breaking terms.

A. Random phase approximation

The collective modes of the system are studied in the random phase approximation (RPA) [34]. They are obtained from the equations of motion of the operators $G_{\alpha\beta}$, which are given by

$$i\partial_t G_{\alpha\beta}^{i,\delta} = [G_{\alpha\beta}^{i,\delta}, \mathcal{H}]. \quad (39)$$

The commutator in this expression contains products of operators on different bonds (i,δ) . These products are decoupled in a mean-field fashion, yielding a set of coupled linear differential equations. After a transformation to frequency- and momentum-space, it takes the form

$$\omega G_{\alpha\beta}(\vec{k}, \omega) = \sum_{\alpha'\beta'} M_{\alpha\beta}^{\alpha'\beta'}(\vec{k}) G_{\alpha'\beta'}(\vec{k}, \omega). \quad (40)$$

The dispersion-relations of the collective modes are obtained from the eigenvalues of the dynamical matrix M ,

while its eigenvectors give the operators which generate these modes.

There is a problem with the above decoupling in the spin-ordered phases. As was discussed in section IV, the low-energy fluctuations of the spin-system behave differently at large J_F and near the spin-disordering transition. For $J_F \ll 1$, the spins around each square plaquette are locked into a symmetric state, forming one spin-2 object, and the low-energy deformations of the spin-state are localized on the antiferromagnetic bonds. The above decoupling, which cuts across the ferromagnetic bonds, then becomes very poor. Near the spin-disordering transition, the spins are rigidly coupled along the antiferromagnetic bonds and the low-energy transversal fluctuations are localized on the ferromagnetic bonds. In this case, the decoupling works well.

The cross-over to spin-2 behavior at large J_F is driven by the \mathcal{H}_1 spin-spin interaction term, Eq.(34). To avoid it, we calculate the mode-spectrum of the Hamiltonian from which this term has been subtracted. The resulting dynamical matrices are listed in appendix B. Subtracting \mathcal{H}_1 makes no difference for the spin-disordered phases, but does change the results in the AF and AFSC phase (we discuss in what way). The \mathcal{H}_1 term breaks $SO(5)$ symmetry, though retaining it at the mean-field level. As a result, the model which we study in RPA has a projected $SO(5)$ symmetry at the tricritical point with fine-tuned t_2 .

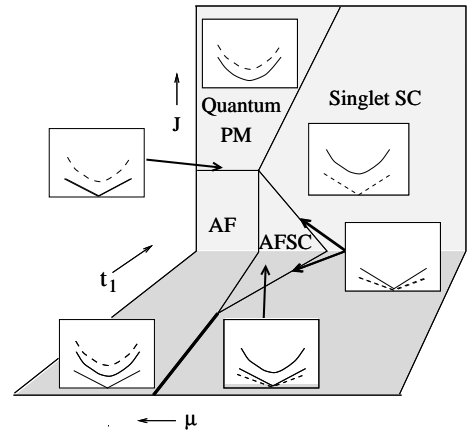


FIG. 7. Sketch of the mode-spectrum in the antiferromagnetic and spin-disordered phases. The dashed lines are pairing modes when gapped (insulating phases) and phase Goldstone modes when acoustic (superconducting phases).

B. mode-spectrum

We briefly discuss the mode-spectrum of the antiferromagnetic and spin-disordered phases. These results are summarized in Fig. 7.

The quantum paramagnet, for which both spin- and gauge-symmetry are unbroken, has no Goldstone modes.

Its spectrum consists of a gapped three-fold degenerate spin-1 magnon mode and a pairing mode which is also gapped. The pairing gap closes at the transition to the singlet superconductor. Precisely at the transition, this mode has a quadratic dispersion. As the hole-pair density is increased from zero, it acquires a finite velocity, becoming the phase Goldstone mode of the superconducting state. This is the behavior expected at a dilute boson transition [32], of which this is a particular example (where the hole-pairs are the dilute bosons). The three-fold degenerate mode of the quantum paramagnet remains gapped through the transition to the superconductor.

The insulating antiferromagnet has a two-fold degenerate spin-wave mode. In addition, it has a gapped mode related to spin-amplitude modulations and a gapped pairing mode. The spin-amplitude mode becomes degenerate with the acoustic spin-wave modes at the transition to the quantum paramagnet, where they turn into the spin-1 magnon triplet. This transition is in the same class as the spin-disordering transition of the Heisenberg bilayer model [33]. The pairing gap closes at the transition to the antiferromagnetic superconductor, where it becomes the acoustic phase Goldstone mode at finite dopings. The spin-amplitude mode remains gapped through the insulator to superconductor transition, but becomes degenerate with the acoustic spin-wave modes at the subsequent transition to the singlet superconductor. At this transition line, the system therefore has four acoustic modes, of which three are degenerate.

C. π -modes

The mode-spectrum as outlined above can be understood entirely from a decoupled perspective of the spin and the phase-sector. At the transition line from insulator to superconductor, the pairing mode softens and continuously acquires a finite velocity. At the transition from a phase with AF order to a spin-disordered phase, the spin-amplitude mode becomes degenerate with the acoustic spin-wave modes. These two effects combined yield the described behavior, and in particular the occurrence of four acoustic modes at the AFSC to Singlet SC transition. This decoupled perspective is correct for $t_2 = 0$. In this case, the gapped modes in the Singlet SC state are indeed spin-1 magnons, as they are in the quantum paramagnet, while the gapped mode in the AFSC is indeed a pure spin-amplitude mode, as it is for the AF insulator.

The t_2 -process, however, provides a coupling between the movement of the hole pairs and the dynamics of the spin-system. This coupling changes the nature of the gapped modes in the superconducting phases with respect to those in their insulating parent-phase. In the AFSC phase, the spin-amplitude mode is mixed

with fluctuations between the hole-pair and the zero-magnetization electron-pair states. In the Singlet SC phase, π -modes (hole-pair to triplet fluctuations) are mixed into the spin-1 magnons.

Close to the transition from the Singlet to the antiferromagnetic SC, the gapped mode becomes degenerate with the acoustic spin-wave modes and the t_2 -process begins to affect the low-energy physics of the system. From the analogy with the spin-disordering transition in the insulating phase, one would expect to find a three-fold degenerate acoustic magnon-mode at this transition (in addition to the phase mode). Instead, the RPA-analysis yields an eigenvector

$$4t_2\sqrt{J-2}(G_{0V} - G_{V0}) + (J - 8t_2)(1 - 2t_1 + 2t_2)(G_{0A} - G_{A0}), \quad (41)$$

which has both a magnon and a π -mode component. Note that this result does not change if the more natural spin-spin interactions, with \mathcal{H}_1 , are used, since \mathcal{H}_1 does not affect the collective modes in the singlet SC phase.

For $J \rightarrow 2$, the spin-disordering line in the superconducting phase approaches half-filling. In this case, Eq.(41) becomes a pure magnon-mode, which is the result expected for the insulating phase. The same eigenvector is found for $t_2 = 0$, which implies that the transition in the superconducting phase is, for that case, indeed of the same type as for the insulators. The π -modes are mixed in for finite t_2 . We find a pure π -mode for $t_2 = J/8$ and $t_1 - t_2 = 1/2$. The first condition is satisfied at the point where the AFSC, triplet SC and singlet SC meet, at $n \rightarrow 0$ (see Fig.5). This is related to the fact that the $n = 0$ -state and the triplet SC, which are related by a π -rotation, become at that point degenerate in energy. The second condition is of more interest: it is fulfilled if the singlet-pair hopping-process and the Néel-moment interaction enter the Hamiltonian in the projected $SO(5)$ -symmetric form $\vec{N}_P^{i,\delta_1} \cdot \vec{N}_P^{i,\delta_2}$. This is of course the case at the p $SO(5)$ -point, which implies that the Singlet SC phase at this point has the mode-content expected from $SO(5)$ -theory: 4 acoustic modes, of which one is a phase-mode and three are π -modes. It is shown in Ref. [15] that this is generally the case for systems with a projected $SO(5)$ symmetry in the SC phase. The symmetry breaking due to the projection onto the lower Hubbard band shows up in the RPA mode-spectrum by a different velocity for the phase- and the π -modes:

$$v_{\text{phase}}^{SC,pSO(5)} = \sqrt{\frac{4 - J^2}{8}},$$

$$v_{\pi}^{SC,pSO(5)} = \frac{2 + J}{4\sqrt{2}}. \quad (42)$$

The two modes become degenerate at $J=6/5$ ($n=4/5$), but this point does not seem to have any special significance,

The condition $t_1 - t_2 = 1/2$ can also be satisfied at the AFSC to Singlet SC transition away from the point with mean-field $SO(5)$ symmetry. In this case, there are additional terms which break the mean-field $SO(5)$ symmetry, since they tune the system away from the tricritical point, but which do not affect the RPA-modes.

D. Projected $SO(5)$ symmetry

In Ref. [15], the mode-spectrum at the p $SO(5)$ -point was studied for a general direction of the superspin. Two striking results were obtained. In the first place, the system has a two-fold degenerate acoustic mode, whose velocity is independent of doping (i.e., independent of the direction of the $SO(5)$ -order parameter). Secondly, the phase Goldstone mode is not acoustic, but gapless with a quadratic dispersion. It was argued that this last effect is caused by the infinite compressibility of the system at the p $SO(5)$ point, where $\partial\langle n\rangle/\partial\mu$ diverges.

Both results are reproduced in our model. Since the second result is related to the infinite compressibility rather than to $SO(5)$ -symmetry, it always occurs at the tricritical point, also if we tune away from $t_1 = -t_2 = \frac{1}{4}$ while keeping $t_1 = t^*, \mu = \mu_c$. By the same argument, this effect will not disappear if the \mathcal{H}_1 -term is added to the Hamiltonian, since this does not affect the mean-field phase-diagram.

The first result is very sensitive to perturbations. As soon as the tricritical point is tuned away from $t_1 = -t_2 = \frac{1}{4}$, the velocity of the acoustic modes becomes n -dependent. Also the addition of \mathcal{H}_1 to the Hamiltonian destroys this effect. This can be seen by calculating the spin-wave velocity from $c = \sqrt{\rho_s/\chi_\perp}$, using the results obtained in section IV, and evaluating it at the mean-field $SO(5)$ -point. This yields

$$v_s^{MF\ SO(5)} = \sqrt{\frac{(2+J)(J+2-2n)(J+1-n)}{8(J+2n)}}, \quad (43)$$

which has an n -dependence. For the model without \mathcal{H}_1 , the stiffness is given by (see Eq.(21,23))

$$\begin{aligned} \rho_s^{\mathcal{H}-\mathcal{H}_1} &= \frac{2}{N\delta\phi^2}\Delta E(\alpha=0) \\ &= n(1-n)(t_1+t_2)(1-\cos 2\chi) + \frac{n^2}{4}(1-\cos^2 2\chi), \end{aligned} \quad (44)$$

where n and χ have the mean-field values listed in table 1. The susceptibility is obtained by multiplying the J_F -term in the mean-field energy Eq.(15) with a factor $\cos^2 \hat{\phi}^y$, adding the magnetic field term Eq.(16), and minimizing with respect to $\hat{\phi}^y$. We obtain

$$\chi_\perp^{\mathcal{H}-\mathcal{H}_1} = \frac{2n(1-\cos 2\chi)}{J-8t_2(1-n)+n(1-\cos 2\chi)}. \quad (45)$$

At the p $SO(5)$ point, this stiffness and susceptibility reproduce the RPA result $v_s = (2+J)/(4\sqrt{2})$, which is independent of doping. Both the phase-ordering and the spin-ordering energy contribute to the spin-wave velocity in the AFSC phase. As one approaches the p $SO(5)$ point, the doping-dependence of the contribution of the spin-ordering energy is precisely compensated by the opposite doping-dependence of the phase-ordering contribution. Note that the model *with* \mathcal{H}_1 yields the same v_s at the transition to the Singlet SC, where $n = (2+J)/4$, see Eq. (43). This demonstrates the insensitivity of the RPA mode-spectrum in the Singlet SC phase to the specific form of the spin-spin interactions.

At the p $SO(5)$ point of our model, the acoustic modes are no longer pure spin-wave, but a combination of spin-wave and π -mode. Their eigenvector is given by

$$\sqrt{1-n}(G_{1V} + G_{V-1}) + \sqrt{n-n_c}(G_{10} + G_{0-1}), \quad (46)$$

which starts out as a spin-wave at half-filling, but crosses over to a π -mode at $n = n_c$. This agrees with Zhang *et al.*'s interpretation of the doping-independent velocity in terms of the projected $SO(5)$ symmetry [15].

VII. SUMMARY

We have introduced a strong coupling model for spin-ordering and superconductivity. The microscopic building blocks of this model are nearest-neighbor electron pairs. The spatial structure of these pairs gives rise to d-wave superconductivity. At the same time, it allows the pairs to have a non-zero uniform or staggered magnetic moment. In order to avoid problems related to dimer-type spatial correlations between the pairs, the model is formulated on a 1/5-depleted lattice. A rich mean-field phase-diagram is obtained, exhibiting in particular a phase which is at the same time an antiferromagnet and a superconductor. The second order lines separating this phase from the antiferromagnetic insulator and the spin-disordered superconductor end at a tricritical point, where the antiferromagnet to superconductor phase-transition becomes first order. By mapping the spin-sector in the antiferromagnetic phases onto a non-linear sigma model, the main corrections to the mean-field phase-diagram have been obtained.

For a specific value of one of the model parameters, a mean-field $SO(5)$ symmetry between the antiferromagnetic and superconducting order-parameter appears to be realized at the tricritical point. It turns out that the model still contains spatial gradient terms which break $SO(5)$ symmetry. These can be removed by modifying the spin-spin interactions. The remaining $SO(5)$ symmetry-breaking is then a pure quantum-effect, being related to the operator-algebra rather than the Hamiltonian. It is shown that true $SO(5)$ symmetry can be realized for this model by allowing double site-occupancy and

fine-tuning the Hubbard U . The approximate symmetry at large U is therefore a projected $SO(5)$ symmetry of the kind discussed in Ref. [15].

We investigated the mode-spectrum using the random phase approximation. It is found that the inter-sublattice hopping process gives rise to the appearance of a π -component in the gapped modes of the Singlet SC phase. Approaching the point with projected $SO(5)$ symmetry from the Singlet SC phase, a three-fold degenerate acoustic π -mode is found as well as an acoustic phase-mode. The RPA mode-spectrum then has the properties expected for an $SO(5)$ -symmetric system in the pure superconducting phase, apart from the fact that the π -modes and the phase-mode have different velocities.

As reported in Ref. [15], the system at the $pSO(5)$ point has a gapless phase-mode with a quadratic dispersion, as well as a two-fold degenerate acoustic mode whose velocity is independent of doping. This acoustic mode crosses over from a pure spin-wave at half-filling to a π -mode at the transition to the Singlet SC phase. We find that the quadratic phase-mode is a property of the tricritical point rather than of the projected $SO(5)$ symmetry. The doping-independent velocity, however, is a strong signature of projected $SO(5)$ symmetry, which can be destroyed even by additional symmetry-breaking terms that leave the mean-field $SO(5)$ symmetry intact.

Acknowledgements. Financial support was provided by the Foundation of Fundamental Research on Matter (FOM), which is sponsored by the Netherlands Organization of Pure research (NWO). JZ acknowledges support by the Dutch Academy of Sciences (KNAW).

APPENDIX A: THE $SO(5)$ ALGEBRA.

A short overview is given of the representation of the $SO(5)$ -algebra for this model.

In the unprojected Hilbertspace, a representation of the $SO(5)$ algebra can be defined which transforms the superspin \vec{N} as a vector. The superspin is given by

$$\vec{N} = \left(\text{Re}\Delta, \vec{\tilde{S}}, \text{Im}\Delta \right), \quad (\text{A1})$$

where

$$\Delta^\dagger = \sqrt{2}(G_{DA} - G_{AV}) \quad (\text{A2})$$

and $\text{Re}\Delta = \frac{1}{2}(\Delta^\dagger + \Delta)$, $\text{Im}\Delta = \frac{1}{2i}(\Delta^\dagger - \Delta)$. The generators of the $SO(5)$ -algebra satisfy the commutation relation

$$[L_{ab}, L_{cd}] = i(\delta_{ac}L_{bd} + \delta_{bd}L_{ac} - \delta_{ad}L_{bc} - \delta_{bc}L_{ad}), \quad (\text{A3})$$

where the indices take the values 1 through 5. The L_{ab} are anti-symmetric under an interchange of a and b . They are given by [11]

$$L_{ab} = \begin{pmatrix} 0 & & & & & \\ 2\text{Re}\pi_x & 0 & & & & \\ 2\text{Re}\pi_y & -S^z & 0 & & & \\ 2\text{Re}\pi_z & S^y & -S^x & 0 & & \\ Q & 2\text{Im}\pi_x & 2\text{Im}\pi_y & 2\text{Im}\pi_z & 0 & \end{pmatrix} \quad (\text{A4})$$

where the π -operators read $\pi_\alpha^\dagger = -\frac{1}{2}c_1^\dagger\sigma_\alpha\sigma_y c_2^\dagger$, with $\vec{\sigma}$ the Pauli matrices [31]. Projecting onto the paired-electron states, we obtain

$$\begin{aligned} \pi_x^\dagger &= \frac{1}{2i}(G_{D1} - G_{D-1} + G_{1V} - G_{-1V}), \\ \pi_y^\dagger &= \frac{1}{2}(G_{D1} + G_{D-1} - G_{1V} - G_{-1V}), \\ \pi_z^\dagger &= \frac{i}{\sqrt{2}}(G_{D0} + G_{0V}). \end{aligned} \quad (\text{A5})$$

The charge-operator is given by

$$Q = n_D - n_V. \quad (\text{A6})$$

It can be checked that \vec{N} indeed transforms as a vector under this $SO(5)$ -algebra:

$$[L_{ab}, N_c] = i(\delta_{ac}N_b - \delta_{bc}N_a), \quad (\text{A7})$$

and furthermore that

$$[N_a, N_b] = iL_{ab}. \quad (\text{A8})$$

APPENDIX B: DYNAMICAL MATRICES

A staggering factor for the antiferromagnetic spin- and the d-wave phase-order has been absorbed into the operators $G_{\alpha\beta}$. After subtraction of \mathcal{H}_1 , the Hamiltonian takes the form of a model on the square lattice, where the operators $G_{\alpha\beta}$ act on the states on the lattice sites. The Singlet dSC, AF dSC, quantum paramagnet and AF insulator mean-field states are all uniform in terms of these operators. It is therefore not necessary to introduce a multi-sublattice structure. The different modes in terms of the real (non-staggered) operators are simply related to the ones obtained here by a shift in k -space.

The operators $G_{\alpha\beta}$ separate into three sets. Each operator couples only to operators in the same set through its RPA equation of motion. One set is formed by the raising operators $\{G_{1V}, G_{1A}, G_{10}, G_{V-1}, G_{A-1}, G_{0-1}\}$, another by the lowering operators, which are related to this set by hermitian conjugation. The third set contains the operators which act only on the zero-magnetization states: $\{G_{AV}, G_{0V}, G_{A0}, G_{VA}, G_{V0}, G_{0A}, n_A, n_0, n_V\}$.

The dynamical matrix of the raising operators has the form

$$M_R = \begin{pmatrix} A^T & B^T \\ -B^T & -A^T \end{pmatrix}, \quad (\text{B1})$$

where A and B are the 3×3 matrices

$$A = \begin{pmatrix} 4\Sigma_t s_\theta^2 \gamma_k + \mu - \frac{J}{4} & -2s_{2\theta} c_\chi (\Delta_t - \frac{\gamma_k}{4}) & \Sigma_t 2s_{2\theta} s_\chi \\ 2s_{2\theta} c_\chi (\Sigma_t \gamma_k - \Delta_t) & c_\theta^2 c_\chi^2 \gamma_k - J & c_\theta^2 s_{2\chi} \\ 2\Sigma_t s_{2\theta} s_\chi (1 - \gamma_k) & \frac{1}{2} c_\theta^2 s_{2\chi} (2 - \gamma_k) & 0 \end{pmatrix}, \quad (\text{B2})$$

$$B = \begin{pmatrix} 0 & \frac{1}{2} s_{2\theta} c_\chi \gamma_k & 0 \\ 0 & c_\theta^2 c_\chi^2 \gamma_k & 0 \\ 0 & -\frac{1}{2} c_\theta^2 s_{2\chi} \gamma_k & 0 \end{pmatrix}, \quad (\text{B3})$$

where we have used the notation

$$\begin{aligned} s_x &= \sin x; \quad c_x = \cos x, \\ \Sigma_t &= t_1 + t_2; \quad \Delta_t = t_1 - t_2, \\ \gamma_k &= \frac{1}{2} (\cos(\vec{k} \cdot \vec{e}_1) + \cos(\vec{k} \cdot \vec{e}_2)), \end{aligned} \quad (\text{B4})$$

with \vec{e}_1 and \vec{e}_2 the basis-vectors of the square lattice spanned by the long bonds, Fig. 1. The angles χ and θ are the ones appearing in the mean field energy Eq.(15). In the insulating phases, θ vanishes, while χ is equal to zero in the spin-disordered phases.

The dynamical matrix of the lowering modes is the same as M_R , apart from a minus sign. The last set has a dynamical matrix

$$M_0 = \begin{pmatrix} C & D^T & E^T \\ -D^T & -C & -E^T \\ F & -F & 0 \end{pmatrix}, \quad (\text{B5})$$

which consists of the 3×3 matrices

$$\begin{aligned} C_{11} &= -4\Delta_t (c_\chi^2 c_\theta^2 - s_\theta^2) \gamma_k + \mu + \frac{3}{4} J \\ C_{12} &= 2\Delta_t c_\theta^2 s_{2\chi} \gamma_k - c_\theta^2 s_{2\chi} \\ C_{13} &= -2s_{2\theta} s_\chi (\Delta_t \gamma_k - \Sigma_t) \\ C_{21} &= 2\Sigma_t c_\theta^2 s_{2\chi} \gamma_k - c_\theta^2 s_{2\chi} \\ C_{22} &= -4\Sigma_t (c_\theta^2 s_\chi^2 - s_\theta^2) \gamma_k + \mu - \frac{J}{4} \\ C_{23} &= 0 \\ C_{31} &= 2\Sigma_t s_{2\theta} s_\chi - \frac{1}{2} s_{2\theta} s_\chi \\ C_{32} &= \frac{1}{2} s_{2\theta} c_\chi \gamma_k \\ C_{33} &= -c_\theta^2 c_{2\chi} \gamma_k + J \end{aligned} \quad (\text{B6})$$

$$D = \begin{pmatrix} 0 & 0 & \frac{1}{2} s_{2\theta} s_\chi \gamma_k \\ 0 & 0 & 2\Delta_t s_{2\theta} c_\chi - \frac{1}{2} s_{2\theta} c_\chi \gamma_k \\ 0 & -2s_{2\theta} c_\chi (\Delta_t - \Sigma_t \gamma_k) & c_\theta^2 c_{2\chi} \gamma_k \end{pmatrix} \quad (\text{B7})$$

$$E = \begin{pmatrix} -2\Delta_t s_{2\theta} c_\chi (1 - \gamma_k) & 0 & c_\theta^2 s_{2\chi} \\ 0 & 2\Sigma_t s_{2\theta} s_\chi (1 - \gamma_k) & -c_\theta^2 s_{2\chi} \\ 2\Delta_t s_{2\theta} c_\chi (1 - \gamma_k) & -2\Sigma_t s_{2\theta} s_\chi (1 - \gamma_k) & 0 \end{pmatrix} \quad (\text{B8})$$

$$F = \begin{pmatrix} -2\Delta_t s_{2\theta} c_\chi & 0 & c_\theta^2 s_{2\chi} \\ 0 & 2\Sigma_t s_{2\theta} s_\chi & -c_\theta^2 s_{2\chi} \\ 2\Delta_t s_{2\theta} c_\chi & -2\Sigma_t s_{2\theta} s_\chi & 0 \end{pmatrix} \quad (\text{B9})$$

For the Singlet SC phase ($\chi = 0$), the operators $G_{\alpha\beta}$ with α and β referring to triplet states decouple from the equations of motion, since there is no longer a triplet component in the mean-field groundstate. This leaves the raising set $\{G_{1V}, G_{1A}, G_{V-1}, G_{A-1}\}$ and the hermitian conjugate lowering set. The set of zero-magnetization operators splits into the transversal set $\{G_{0V}, G_{0A}, G_{V0}, G_{A0}\}$ and the longitudinal set $\{G_{AV}, G_{VA}, n_A - n_V\}$. The dynamical matrices of the first three sets contain the three-fold degenerate π - and spin-1 magnon modes. The fourth set contains the phase and the pairing mode.

In the quantum paramagnet phase ($\chi = \theta = 0$), the first three sets further simplify. Since the π -operators do not refer to the spin-singlet groundstate, only the spin-1/charge-0 operators are left in these sets. The phase-mode $n_A - n_V$ disappears from the last set.

-
- [1] P. Nozieres, S. Schmitt-Rink, J. Low-Temp. Phys. **59**, 159 (1985).
 - [2] J. R. Engelbrecht, A. Nazarenko, M. Randeria and E. Dagotto, Phys. Rev. B **57**, 13406 (1998).
 - [3] Ch. Renner *et al.*, Phys. Rev. Lett. **80**, 3606 (1998).
 - [4] V. J. Emery and S. A. Kivelson, Nature **374**, 434 (1995).
 - [5] D. Pines, Proc. of Euroconf. on 'Correlations in Unconventional Quantum Liquids', Erova, Portugal, Oct. 1996; cond-mat/9702187.
 - [6] J. M. Tranquada *et al.*, Nature **375**, 561 (1995)
 - [7] G. M. Luke *et al.*, Hyp. Int. **105**, 113 (1997); W. Wagener *et al.*, Phys. Rev. B **55**, R14761 (1997).
 - [8] H. Kimura *et al.*, Phys. Rev. B **59**, 6517 (1999).
 - [9] J. M. Tranquada *et al.*, Phys. Rev. Lett. **78**, 338 (1997).
 - [10] A. H. Castro-Neto and D. Hone, Phys. Rev. Lett. **76**, 2165 (1996); C. N. A. van Duin and J. Zaanen, Phys. Rev. Lett. **80**, 1513 (1998); S. Sachdev, Phys. World **12**, 33 (1999).
 - [11] S. C. Zhang, Science **275**, 1089 (1997).
 - [12] J. Zaanen, Physica C **318**, 217 (1999).
 - [13] M. Vojta and S. Sachdev, cond-mat/9906104.
 - [14] R. Eder *et al.*, Phys. Rev. B **59**, 561 (1999).
 - [15] S. C. Zhang *et al.* cond-mat/9904142.
 - [16] G. Sierra *et al.*, Phys. Rev. B **57**, 11666 (1998); M. Troyer, H. Tsuretsugu, T. M. Rice, Phys. Rev. B **53**, 251 (1996).

- [17] D. Rokhsar and S. Kivelson, Phys. Rev. Lett. **61**, 2376 (1988).
- [18] E. Fradkin and S. Kivelson, Mod. Phys. Lett. **B4**, 225 (1990).
- [19] P. W. Kasteleyn, Physica **27**, 1209 (1961).
- [20] R. Micnas, J. Ranninger and S. Robaszkiewicz, Rev. Mod. Phys. **62**, 113 (1990).
- [21] C. N. A. van Duin and J. Zaanen, Phys. Rev. Lett. **78**, 3019 (1997).
- [22] A. van Otterlo *et al.*, Phys. Rev. B **52**, 16176 (1995).
- [23] F.D.M. Haldane, Phys. Lett. **93 A**, 464 (1983), Phys. Rev. Lett. **50**, 1153 (1983).
- [24] S. Chakravarty, B. I. Halperin and D. R. Nelson, Phys. Rev. Lett. **60**, 1057 (1988); *ibid.* Phys. Rev. B **39**, 2344 (1989).
- [25] J. Igarashi, Phys. Rev. B **46**, 10763 (1992).
- [26] G. Aeppli *et al.* Science **278**, 1432 (1997).
- [27] V. Barzykin and D. Pines, Phys. Rev. B **52**, 13585 (1995); Y. Zha, V. Barzykin and D. Pines, cond-mat/9601016.
- [28] A.V. Chubukov, S. Sachdev and J. Ye, Phys. Rev. B. **49**, 11919 (1994).
- [29] E. W. Carlson, S. A. Kivelson, V. J. Emery and E. Manousakis, cond-mat/9902077.
- [30] S. C. Zhang, Proceedings of the Grand Finale Taniguchi Symposium on “The Physics and Chemistry of Transition Metal Oxides”; cond-mat/9808309 (1998).
- [31] D. Scalapino, S. C. Zhang and W. Hanke, Phys. Rev. B **58** 443 (1998).
- [32] S. Sachdev Quantum Phase Transitions, to be published by Cambridge University Press.
- [33] A. V. Chubukov and D. K. Morr, Phys. Rev. B **52**, 3521 (1995).
- [34] S.B. Haley and P. Erdős, Phys. Rev. B **5**, 1106 (1972).